Journal Name

Cite this: DOI: 10.1039/c0xx00000x

www.rsc.org/xxxxxx

ARTICLE TYPE

Fine Tuning and Orientation Control of Surface Cu Complexes on TiO_2(110) Premodified with Mercapto Compounds: the Effect of Different Mercapto Group Positions

Satoru Takakusagi,*[a] Hirotaka Nojima, [a] Hiroko Ariga, [a] Hiromitsu Uehara, [a] Kotaro Miyazaki, [a] Wang-Jae Chun, [b] Yasuhiro Iwasawa [c] and Kiyotaka Asakura*[a]

Received (in XXX, XXX) Xth XXXXXXXXX 20XX, Accepted Xth XXXXXXXXX 20XX
DOI: 10.1039/b000000x

Three-dimensional structures of vacuum-deposited Cu species formed on TiO_2(110) surfaces premodified with three mercaptobenzoic acid (MBA) isomers were studied using polarization-dependent total reflection fluorescence X-ray absorption fine structure (PTRF-XAFS) . We explored the possibility of fine tuning and orientation control of the surface Cu structures, including their coordination and configuration against the surface, according to the different mercapto group positions of the three MBA isomers (*o*-, *m*-, and *p*-MBA). Almost linear S-Cu-O (lattice O of TiO_2) surface compounds were formed on the three MBA-modified TiO_2(110) surfaces; however, the orientation of the Cu species on the *o*- and *m*-MBA-modified TiO2(110) surfaces (40-45° inclined from the surface normal) was different from that on the *p*-MBA-modified TiO2(110) surface (60° from the surface normal). This work suggests that the selection of a different MBA isomer for premodification of a single crystal TiO_2(110) surface enables fine tuning and orientation control of surface Cu complexes.

1. Introduction

Many heterogeneous catalysts are used as supported metal catalysts for the preparation of highly dispersed metal active phases. To achieve a high dispersion, the metal species should be bound strongly to the support surface. The immobilization of metal species through covalent bonding can provide highly dispersed metal species, more so than the metal ion impregnation or ion exchange methods. The immobilized metal species is itself an active structure or is converted to an active structure after appropriate treatment.[1] The immobilization of metal species is achieved by the grafting of a metal complex onto an oxide surface by the reaction with OH groups or by the anchoring of a metal species through a linker molecule that strongly interacts with both the metal species and support.[1] The structures and oxidation states of the surface metal species can be determined and controlled at the atomic level; however, it is difficult to determine and tune the three-dimensional structure of a surface metal species, such as its orientation, coordination and configuration with respect to the support surface, by which the synergistic effect between the metal species and support can be controlled at the atomic level. A single crystal oxide surface is a promising candidate for achieving this purpose, because conventional powder support materials have ill-defined surfaces, so that three-dimensional structural analysis and tuning is not applicable. Polarization-dependent total reflection fluorescence X-ray absorption fine structure (PTRF-XAFS) analysis can provide three-dimensional structural information about the region around highly dispersed metal species on single crystal surfaces.[2] We have determined the three-dimensional structures of Cu, Co, Pt and Mo complexes and their derivatives grafted onto SiO_2(0001), Al_2O_3(0001) and TiO_2(110) in order to elucidate the metal-support interactions at the atomic level.[3-8]

Grafting methods typically require the preparation of organometallic compounds in advance, although these compounds are often unstable in air or high temperature. However, if the oxide support surface is premodified with an organic ligand that strongly anchors to a metal atom through a covalent bond, then a well-defined atomic metal species can be obtained without the need for organometallic compounds. We have successfully prepared an atomically dispersed Cu–thiophene compound with Cu-S bond simply by vacuum deposition of Cu on a TiO_2(110) surface that was premodified with thiophene carboxylic acid (TCA) in which the carboxylic group acted as a binding part to the TiO_2 substrate.[9] This preparation method is referred to as the premodified surface method, in which various organic compounds are available for premodification purposes and for selective fine tuning of the surface metal structures. and for selective fine tuning of the surface metal structures.

In this work, the TiO_2(110) surface was premodified with mercaptobenzoic acid (MBA) isomers to attempt fine tuning and orientation control of surface metal (Cu) structures, including their coordination and configuration against the TiO_2(110) support. Fine tuning and orientation control of metal species on an oxide support surface are important to modify the metal-support interaction that largely affects their catalytic properties and electron transfer processes from the metal (support) to the support (metal). MBA has three isomers, i.e., *o*-, *m*- and *p*-MBA, which have different merapto group distances from the surface, where the S atom position influences the structure of the Cu species. Compared with the TCA molecule used in the previous study,[9] the position of the S atom in MBA can be controlled more precisely, because MBA has more isomers than TCA, and the S atom of the mercapto group has a higher affinity to metal atoms

than that of thiophene, and thus, many more examples of metal-thiolate compounds are reported than metal-thiophene compounds. Figure 1 shows that the distance between the S atom of the mercapto group and fivefold-coordinate Ti^{4+} on the support surface changes from 0.40 to 0.87 nm[10-13] and, therefore, the structure of vacuum-deposited Cu species on different MBA–modified TiO_2(110) is expected to differ according to the S position. The three-dimensional structures of the Cu species on different MBA-modified TiO_2(110) surfaces are determined using PTRF-XAFS, and the origin of the different Cu structures is discussed.

2. Experimental

2-1 Sample preparation

Optically polished Nb-doped (0.05 wt%) TiO_2(110) substrate samples (20×20×1 mm^3, Furuuchi Co., Japan) were cleaned by immersion in 10% HF solution for 10 min, followed by annealing in air at 700 ℃ for 1 h, in accordance with previously reported methods.[14,15] MBA has a low vapor pressure, which causes difficulty if premodification of the TiO_2(110) surface is attempted with MBA vapor. Therefore, a wet chemical process was applied for premodification of the TiO_2(110) surface. The process is simple and can extend the applicability of many other functional organic compounds employed for support surface premodification. The cleaned support surface was first immersed in a 1 mM ethanol solution of *o*-MBA (Toronto Research Chemicals Inc, Canada), *m*-MBA (Toronto Research Chemicals Inc, Canada) or *p*-MBA (Wako Pure Chemical Industries, Ltd., Japan) for 24 hours to modify the TiO_2(110) surface with the corresponding MBA monolayer. Formation of the MBA monolayer was confirmed by spectroscopic ellipsometry (GES5E, Semilab) and typical results are shown in Figure S1(a) and (b) in Supplementary Information. The substrate sample was then transferred to an ultra-high vacuum (UHV) PTRF-XAFS chamber[16] and Cu was evaporated onto the MBA-modified TiO_2(110) surface by resistive heating of a tungsten filament wrapped with Cu wire (99.999% purity, Nilaco Co., Japan). The Cu coverage was estimated to be 0.35±0.1 ML (monolayer) from the X-ray photoelectron spectroscopy (XPS) peak area ratios of $Cu2p_{3/2}$-$Ti2p_{3/2}$. 1 ML was defined as 5.2×10^{14} /cm^2 with correspondence to the TiO_2(1×1) unit cell.

2-2 PTRF-XAFS measurements

PTRF-XAFS measurements were performed after Cu deposition onto the premodified TiO_2(110) substrate samples without exposure to air, using the UHV PTRF-XAFS chamber at BL9A of the Photon Factory at the Institute of Materials Structure Science (KEK-IMSS-PF, Tsukuba, Japan).[17]

The storage ring energy and ring current were 2.5 GeV and 400 mA, respectively. Considering the anisotropic surface structure of TiO_2(110), PTRF-XAFS measurements were conducted with three different orientations against the electric vector (***E***) of the incident X-rays, i.e., two orientations parallel to the surface, ***E***//[001], $[1\bar{1}0]$ and an orientation perpendicular to the surface, ***E***//[110], as reported elsewhere.[5,6,8,9,16,18-20] The polarization dependence of an overall XAFS oscillation $\chi_{obs}(k)$ can be given by equation [21]

$$\chi_{\mathrm{obs}}(k) = 3\sum_i \cos^2\theta_i \chi_i(k) \qquad (1)$$

where θ_i and $\chi_i(k)$ are the angle between the *i*-th bond direction and the electric vector of the X-ray and partial XAFS oscillation accompanying the *i*-th bond, respectively. The Cu Kα fluorescence was detected using a 19-element Ge solid state detector (SSDGL0110S, Canberra, USA). PTRF-XAFS analysis was performed using REX 2000 (Rigaku Co., Japan) for curve fitting analysis and FEFF8.02 code for theoretical simulation of the extended X-ray absorption fine structure (EXAFS) oscillation, $\chi_{cal}(k)$.[22] The goodness of fit between $\chi_{obs}(k)$ and $\chi_{cal}(k)$ was evaluated using:

$$R = \sqrt{\frac{1}{N}\sum_k \frac{(\chi_{obs}(k) - \chi_{cal}(k))^2}{\varepsilon(k)^2}} \qquad (2)$$

where N and $\varepsilon(k)$ are the number of data points and the error, respectively. The structure model was adopted when R values lower than unity were obtained.

3. Results and Discussion

3-1 Cu deposition on the TiO_2(110) surface premodified with *o*-MBA (Cu/*o*-MBA/TiO_2(110))

Figure 2(a) shows polarization-dependent X-ray absorption near edge structure (XANES) spectra for Cu/*o*-MBA/TiO_2(110), and Figure 2(b) shows XANES spectra for Cu reference compounds. The XANES spectra for Cu/*o*-MBA/TiO_2(110) showed different features from that of Cu foil, which suggests the formation of a non-metallic Cu species. The mid-edge features at around 8984 eV for all orientations could be assigned to the $1s \rightarrow 4p\pi^*$ transition, as determined from previous XANES measurements and *ab* initio calculations.[23,24] The inflection points of the edge appeared around 8981 eV for all orientations. Considering that the respective inflection points for Cu foil, Cu_2O, CuO, CuS and $[N(n\text{-}Bu)_4]_2[Cu(mnt)_2]$ (mnt: maleonitriledithiolato ligand) appeared at 8979.5, 8980.6, 8984.5, 8982.8 and 8982.8 eV,[25] the oxidation state of the Cu species formed on the TiO_2(110) surface premodified with *o*-MBA is monovalent. There is a strong polarization dependence, where the largest $1s \rightarrow 4p\pi^*$ peak was found for the [001] direction while the post edge features were stronger for the [110] direction, suggesting orientation of the Cu species is not random but ordered with respect to the TiO_2(110) surface.

Figure 3 shows polarization-dependent EXAFS spectra for Cu/*o*-MBA/TiO_2(110), in addition to spectra for reference compounds. The envelopes of the PTRF-EXAFS oscillations are quickly damped in the higher k region, compared to that for Cu foil. This indicates that the nearest neighbor atom of Cu is not Cu, but a lighter atom such as sulfur or oxygen. The polarization dependence was such that the amplitudes of the EXAFS oscillations in the [001] and $[1\bar{1}0]$ directions were almost equal, but were smaller than that in the [110] direction. A preliminary curve fitting analysis indicated no contribution from Cu-Cu interaction, which suggests that no Cu aggregation occurred, while Cu-S (0.219±0.003 nm) and Cu-O (0.185±0.003 nm) interactions were dominant in the three observed spectra. The Cu-S bond distance was slightly shorter than or comparable with that in $[(N(n\text{-}Bu)_4)][Cu(mnt)_2]$ (0.227-0.229 nm)[26] and CuS (0.219-0.233 nm).[27] Previous results for Cu deposited directly on

a TiO_2(110) surface by vacuum evaporation revealed that Cu was easily aggregated to form particles, even at a very low coverage of 0.03 ML,[28] therefore, Cu aggregation was effectively blocked on the surface by the presence of sulfur atoms in coadsorbed *o*-MBA molecules. The curve fitting analysis also revealed that the effective coordination numbers for Cu-S and Cu-O in the [110] direction were larger (ca. 1.5 times) than those in the [001] and [1$\bar{1}$0] directions.

To determine the accurate structure of the Cu species, an iteration method was employed using a FEFF code and a real-space model structure.[5,6,8,9,16,18-20] We determined the structure based on the following results and knowledge about *o*-MBA and TiO_2(110) surface.

(1) Our polarization-dependent EXAFS measurements in Figure 3(a) determined the locations and orientations of S and O bonded with Cu.

(2) The *o*-MBA molecules adsorbed on the TiO_2(110) with the Ti^{4+}-carboxylate bonding.

(3) The *o*-MBA molecular structure was taken based on the literature.[11]

(4) We confirmed that the adsorbed *o*-MBA molecules were not decomposed or desorbed before and after Cu deposition by XPS measurements, suggesting its molecular structure was preserved.

Figure 4(a) and (b) show the proposed model structure that fulfill all the four conditions mentioned above and polarization-dependent FEFF simulation, respectively. The calculated EXAFS oscillations from the proposed model were in good agreement with the observed spectra. The Cu–S bond distance was 0.219 nm, while that for the Cu–O interaction was 0.185 nm. The Cu–S and Cu–O bond angles to the surface normal were 45 and 43°, respectively, where the precision by FEFF simulation was less than 3°. The S–Cu–O bond angle was estimated to be 177°, which is close to 180°. Many Cu(I) compounds have a linear structure accompanied by two ligands; therefore, it was concluded that Cu was monovalent, as indicated by the XANES result. We also considered structural models with Cu-O (oxygen in the COOH or carboxylate of the MBA) bonding since the oxygen is also reactive and has a possibility to form the S-Cu-O structure. However we could not reproduce the observed polarization-dependent EXAFS spectra in Figure 3(a) by theoretical simulation using the models. Thus we concluded that the oxygen of the S-Cu-O structure was from the TiO_2 substrate.

It has been previously reported[9] that the stable adsorption sites for Cu on a bare TiO_2(110) surface could be atop sites of the bridging oxygens, because a bridging oxygen has a dangling bond pointing upwards from the surface.[29] However, Cu deposited directly on the bare TiO_2(110) surface was aggregated to form clusters.[28] This indicates that the strength of the Cu-bridging oxygen bond is not sufficient to fix the Cu atom. The Cu atom can thus easily migrate to other atop sites of the bridging oxygen atoms until it reaches a Cu island, which results in aggregation to form Cu metal clusters. In contrast, the S atom of *o*-MBA preadsorbed on the TiO_2(110) surface immobilizes the migrating Cu atom in cooperation with the bridging oxygen accompanied by rotation of the bond connecting the COO- moiety and phenyl ring. We propose that the formation of a chemical bond between Cu and S with the bridging oxygen thermodynamically stabilizes the monomeric Cu species. This Cu species is stable even after annealing at 200 °C for 1 hour in UHV (Figure S1(c) and S2(b) in Supplementary Information) and after exposure to air at room temperature (Figure S2(a) in Supplementary Information).

3-2 Cu deposition on the TiO_2(110) surface premodified with *m*-MBA (Cu/*m*-MBA/TiO_2(110))

Figures 5(a) and (b) show polarization-dependent XANES and EXAFS spectra for Cu/*m*-MBA/TiO_2(110), respectively. In Figure 5(a), the inflection points of the absorption edge appeared around 8981 eV for all orientations, which indicates that Cu is not metallic but monovalent, and the largest 1s→4pπ* peak for the [001] direction was also found. The EXAFS spectra had similar features to those of Cu/*o*-MBA/TiO_2(110), in which the envelopes of the PTRF-EXAFS oscillations were quickly damped compared with that for Cu foil, and the amplitude of the EXAFS oscillation in the [110] direction was larger than that for the other two directions. These results indicate that the local structure around Cu is similar to that of Cu/*o*-MBA/TiO_2(110). Curve fitting analysis revealed the presence of Cu-S (0.219±0.03 nm) and Cu-O bonding (0.185±0.003 nm) in all orientations and the ratios of the effective coordination numbers for Cu-S and Cu-O bonds among the three polarization directions were similar to those for Cu/*o*-MBA/TiO_2(110).

Figure 6(a) shows a model structure produced by FEFF simulation that reproduces the observed spectra well (Figure 6(b)). A similar local structure around Cu as that in Cu/*o*-MBA/TiO_2(110) was obtained, i.e., an almost linear S-Cu-O tructure. The Cu–S bond distance was 0.219 nm while that for Cu–O was 0.185 nm. The Cu–S and Cu–O bond angles to the surface normal were 44 and 41°, respectively, where the precision by FEFF simulation was less than 4°. The S–Cu–O bond angle was estimated to be 176°. Note that one Ti-carboxylate bond of the adsorbed *m*-MBA had to be cleaved to give a monodentate adsorption structure so that Cu could form bonds with S and O atoms, which was similar to the case previously reported for Cu/TCA/TiO_2(110).[9] These results indicate that formation of the linear S-Cu-O structure is energetically favored, even though one Ti-carboxylate bond in the adsorbed *m*-MBA was cleaved.

3-3 Cu deposition on the TiO_2(110) surface premodified with *p*-MBA (Cu/*p*-MBA/TiO_2(110))

Figures 7(a) and (b) show polarization-dependent XANES and EXAFS spectra for Cu/p-MBA/TiO_2(110), respectively. In Figure 7(a), the inflection points of the absorption edge appear around 8981 eV in all orientations, which indicates that Cu is not metallic but monovalent. In contrast to the XANES results of Cu/*o*-MBA/TiO_2(110) and Cu/*m*-MBA/TiO_2(110) shown in Figure 2(a) and Figure 5(a), different polarization dependence was observed, where the largest 1s→4pπ* peak was found for the [110] direction, indication a different orientation of the Cu species. As expected, the EXAFS spectra in Figure 7(b) also showed a different polarization dependence from those for Cu/o-MBA/TiO_2(110) and Cu/*m*-MBA/TiO_2(110), in which the amplitude of EXAFS oscillation in the [110] direction is smaller than that in the other two directions. Curve fitting analysis indicates the Cu-S (0.223±0.004 nm) and Cu-O (0.190±0.003 nm) contributions to the observed spectra.

Figure 8(a) and (b) show a proposed model structure and polarization dependent FEFF simulation for Cu/*p*-

MBA/TiO_2(110), respectively. The calculated EXAFS oscillations for the proposed model are in good agreement with The Cu–S and Cu–O bond angles to the surface normal were both 60°, and the S–Cu–O bond angle was estimated to be 180°, where the precision by FEFF simulation was less than 4°. As expected, the Cu-S and Cu-O bonds were more parallel to the surface than those of Cu/*o*-MBA/TiO_2(110) and Cu/*m*-MBA/TiO_2(110), probably due to the limited conformation of adsorbed *p*-MBA to form a bond with Cu attached to the bridging oxygen through sulfur. The Cu-S and Cu-O bond distances were slightly longer than those for Cu/*o*-MBA/TiO_2(110) and Cu/*m*-MBA/TiO_2(110), which may also be due to distortion in the structure arising from the more flat-lying orientation of the Cu-S and Cu-O bonds formed by the Cu species compared with those for Cu/*o*-MBA/TiO_2(110) and Cu/*m*-MBA/TiO_2(110). One Ti-carboxylate bond of the adsorbed *p*-MBA was cleaved, and a monodentate adsorption structure was adopted, similar to that for Cu/*m*-MBA/TiO_2(110). No Cu-Ti interaction with the nearest Ti_N denoted in Figure 8(a) was observed at less than 0.29 nm, which indicates that the bridging oxygen atom bonded with Cu moved upward in the [110] direction by more than 0.040 nm. The upward displacement of the bridging oxygen atom normal to the surface may be induced by interaction with the atomically dispersed Cu species. A previous surface X-ray diffraction study of Cu on TiO_2(110) suggested that the bond length between the bridging oxygen and the nearest Ti atom was increased by 11.9±5.1% (compared to the bulk Ti-O distance) after vacuum deposition of Cu metal,[30] which is in agreement with the present results (14% increase when the upward displacement of the bridging oxygen is 0.040 nm).

The results also indicate that formation of the S-Cu-O structure is strongly favored and that premodification of the TiO_2(110) surface with functional organic molecules containing a mercapto group effectively promotes atomic dispersion of vacuum-deposited Cu metal.

3-4 Effect of different mercapto group positions in preadsorbed MBA molecules on the final Cu structure

We initially expected three possible scenarios for Cu structures on the three MBA-modified TiO_2(110) surfaces with different mercapto group positions (Figure 1). The first scenario is where the vacuum-deposited Cu is anchored to one or two S atoms, while keeping the MBA adsorption structures intact. The TiO_2(110) surfaces premodified with *m*-MBA and *p*-MBA may be candidates for such interaction. The second scenario is where Cu is trapped between the S atom of the MBA and the bridging oxygen atom of the substrate TiO_2(110) surface. According to the adsorbed molecular structure, adsorption of *o*-MBA could realize and stabilize this type of Cu structure. The final scenario is where the interaction between the Cu and S atoms of MBA is weak, so that no strong bond is formed between them. In this case, Cu aggregates to form particles on the *o*-, *m*-, or *p*-MBA-modified TiO_2(110) surfaces, similar to the case for Cu on the bare TiO_2(110) surface.

For all three MBA molecules with different mercapto group positions, the monatomic Cu species was stabilized by bond formation with a sulfur atom of the corresponding MBA and with a bridging oxygen atom of the TiO_2(110) substrate surface to form a linear S-Cu-O structure, which corresponds to the second scenario. It is interesting that the linear S-Cu-O structure can be formed even with adsorbed *m*- and *p*-MBA, although the mercapto group is more distant from the surface (0.71 nm and 0.81 nm above the surface before Cu deposition, respectively). The sulfur atom can become fixed to the diffusing Cu in cooperation with the bridging oxygen, because the linear Cu(I) species is stable and the molecular orientation of adsorbed *m*- and *p*-MBA can change following the equilibrium between bridge-bidentate and monodentate adsorption structures:

m-(or *p*-)MBA (bridge-bidentate)⇆*m*-(or *p*-)MBA (monodentate) (3)

The equilibrium between bridge-bidentate and monodentate carboxylate has been demonstrated by scanning tunneling microscopy (STM) observations of formate on a TiO_2(110) surface.[31]

Considering the final structures of the surface Cu complexes of Cu/*o*-, *m*-, *p*-MBA/TiO_2(110), Cu/*p*-MBA/TiO_2(110) has the lowest thermal stability, because the Cu-S and Cu-O distances are slightly longer than those of the other Cu species. The origin of the longer Cu-S and Cu-O bond distances in Cu/*p*-MBA/TiO_2(110) is the more flat-lying orientation of the bonds (Cu-O bond in particular), because the dangling bond of the bridging oxygen points toward the atop site, which results in less overlap between the Cu and oxygen dangling bond. Although the local structure around the Cu species in Cu/*o*-MBA/TiO_2(110) is almost the same as that in Cu/*m*-MBA/TiO_2(110), Cu in Cu/*o*-MBA/TiO_2(110) may be more stable, because the adsorbed o-MBA can maintain the bridge-bidentate form on the TiO_2(110) surface before and after Cu deposition.

4. Conclusions

Atomically dispersed Cu species were prepared on TiO_2(110) surfaces premodified with *o*-, *m*- or *p*-MBA. The three-dimensional structures of these Cu species were determined using the PTRF-EXAFS technique. S-Cu-O linear structures were formed on all three of the MBA-modified TiO_2(110) surfaces. However, the orientation of the Cu species on the TiO_2(110) surface premodified with *o*- and *m*-MBA was 40-45° inclined from the surface normal, while that on TiO_2(110) premodified with *p*-MBA was more flat at 60° from the surface normal, therefore, we can control orientation of surface Cu structures by using different isomers of MBA. This difference in orientation may modify the synergistic effect of the oxide support on the metal species, which would affect chemical reactivity of the metal species.

ACKNOWLEDGMENT

The authors express their thanks to Prof. M. Nomura and the Photon Factory staff for helpful technical support of XAFS measurements. The authors are also grateful to Prof. K. Ikeda for assistance with spectroscopic ellipsometry measurements. This work was conducted under the approval of the Photon Factory Advisory Committee (Nos. 2012G165, 2010G128, 2010G601, 2008G603). This work was financially supported by the New Energy and Industrial Technology Organization (NEDO)

(Demonstrative Research on Solid Oxide Fuel Cells/Fundamental Technologies Development/Analysis of Structure, Reactions, and Material Transfer of MEA Materials) and MEXT KAKENHI Grant Number 23550001.

Notes and references

[a] *Catalysis Research Center, Hokkaido University, Sapporo, Hokkaido 001-0021, Japan. Fax: +81-706-9114; Tel: +81-706-9114; E-mail: takakusa@cat.hokudai.ac.jp (S.T), askr@cat.hokudai.ac.jp (K.A.)*

[b] *Department of Material Sciences, International Christian University, Mitaka, Tokyo 181-8585, Japan.*

[c] *Department of Engineering Science, The University of Electro-Communications, Chofu, Tokyo 182-8585, Japan.*

† Electronic Supplementary Information (ESI) available: [details of any supplementary information available should be included here]. See DOI: 10.1039/b000000x/

‡ Footnotes should appear here. These might include comments relevant to but not central to the matter under discussion, limited experimental and spectral data, and crystallographic data.

1 F. Averseng, M. Vennat and M. Che, Grafting and Anchoring of Transition Metal Complexes to Inorganic Oxides, in *Handbook of Heterogeneous Catalysis*; Wiley-VCH, 2008, pp. 522-539.

2 K. Asakura, Polarization-dependent Total Reflection Fluorescence Extended X-ray Absorption Fine Structure and its Application to Supported Catalysis, in *Catalysis*, RSC publishing, 2012, pp 281-322.

3 M. Shirai, K. Asakura and Y. Iwasawa, *Chem. Lett.* 1992, 1037-1040.

4 K. Asakura, W.-J. Chun, M. Shirai, K. Tomishige and Y. Iwasawa, *J. Phys. Chem. B*, 1997, **101**, 5549-5556.

5 Y. Tanizawa, T. Shido, W.-J. Chun, K. Asakura, M. Nomura and Y. Iwasawa, *J. Phys. Chem. B*, 2003, **107**, 12917-12929.

6 Y. Tanizawa, W.J. Chun, T. Shido, K. Asakura and Y. Iwasawa, *J. Synchrotron Rad.*, 2001, **8**, 508-510.

7 M. Shirai, T. Inoue, H. Onishi, K. Asakura and Y. Iwasawa, *J. Catal.*, 1994, **145**, 159-165.

8 K. Asakura, W.-J. Chun and Y. Iwasawa, *Jpn. J. Appl. Phys.* 1999, **38-1**, 40-43.

9 W.-J. Chun, Y. Koike, K. Ijima, K. Fujikawa, H. Ashima, M. Nomura, Y. Iwasawa and K. Asakura, *Chem. Phys. Lett.* 2007, **433**, 345-349.

10 P. Käckella and K. Terakura, *Surf. Sci.*, 2000, **461**, 191-198.

11 T. Steiner, *Acta Cryst. C*, 2000, **56**, 876-877.

12 C.E. Rowland, N. Belai, K.E. Knope and C. L. Cahill, *Cryst. Growth Des*. 2010, **10**, 1390-1398.

13 U. Helmstedt, S. Lebedkin, T. Höcher, S. Blaurock and E. Hey-Hawkins, *Inorg. Chem*. 2008, **47**, 5815-5820.

14 R. Nakamura, N. Ohashi, A. Imanishi, T. Osawa, Y. Matsumoto, H. Koinuma and Y. Nakato, *J. Phys. Chem. B*, 2005, **109**, 1648-1651.

15 Y. Yamamoto, K. Nakajima, T. Ohsawa, Y. Matsumoto and H. Koinuma, *Jpn. J. Appl. Phys.* 2005, **44**, L 511–L 514.

16 W.-J. Chun, Y. Tanizawa, T. Shido, Y. Iwasawa, M. Nomura and K. Asakura, *J. Synchrotron Rad.*, 2001, **8**, 168-172.

17 M. Nomura and A. Koyama, *J. Synchrotron Rad.* 1999, **6**, 182-184.

18 Y. Koike, K. Ijima, W.-J. Chun, H. Ashima, T. Yamamoto, K. Fujikawa, S. Suzuki, Y. Iwasawa, M. Nomura and K. Asakura, *Chem. Phys. Lett.*, 2006, **421**, 27-30.

19 Y. Koike, K. Fujikawa, S. Suzuki, W.J. Chun, K. Ijima, M. Nomura, Y. Iwasawa and K. Asakura, *J. Phys. Chem. C*, 2008, **112**, 4667-4675.

20 W.-J. Chun, Y. Koike, H. Ashima, K. Kinoshita, K. Ijima, K. Fujikawa, S. Suzuki, M. Nomura, Y. Iwasawa and K. Asakura, *Chem. Phys. Lett.*, 2009, **480**, 99-102.

21 M. Shirai and Y. Iwasawa, X-ray Absorption Fine Structure for Catalysts and Surfaces; World Scientific, Singapore, 1996.

22 A.L. Ankudinov, B. Ravel, J.J. Rehr and S.D. Conradson, *Phys. Rev. B*, 1998, **58**, 7565-7576.

23 N. Kosugi, H. Kondoh, H. Tajima and H. Kuroda, *Chem. Phys.*, 1989, **135**, 149-160.

24 T. Yokoyama, N. Kosugi and H. Kuroda, *Chem. Phys.*, 1986, **103**, 101-109.

25 The inflection point values of the reference compounds reported here are slightly different from those in Ref. 9, due to the use of different background subtraction functions; however, the same tendency to increase with higher Cu oxidation states was observed.

26 K.W. Plumlee, B.M. Hoffman and J.A. Ibers, *J. Chem. Phys.*, 1975, **63**, 1926-1942.

27 H. T. Evans and J. A. Konnert, *Amer. Mineral.*, 1976, **61**, 996-1000.

28 D. A. Chen, M.C. Bartelt, R. Q. Hwang and K.F. McCarty, *Surf. Sci.*, 2000, **450**, 78-97.

29 K. Ding, J. Li, K. Ding and Y. Zhang, *J. Mol. Struct.: THEOCHEM*, 2005, **728**, 123-127.

30 G. Charlton, P.B. Howes, C.A. Muryn, H. Raza, N. Jones, J.S.G. Taylor, C. Norris, R. McGrath, D. Norman, T.S. Turner and G. Thornton, *Phys. Rev. B*, 2000, **61**, 16117-16120.

31 M. Aizawa, Y. Morikawa, Y. Namai, H. Morikawa and Y. Iwasawa, *J. Phys. Chem. B*, 2005, **109**, 18831-18

Figure Captions

Figure 1 Structural models of (a) *o*-MBA, (b) *m*-MBA and (c) *p*-MBA adsorbed on a TiO_2(110) surface. Ti_{5c} denotes fivefold-coordinated Ti^{4+} of the TiO_2(110) surface. The distance of the S atom to the Ti_{5c} was estimated from the previous reports that are theoretical calculation of adsorbed structure of formate on the TiO_2(110) surface[10] and crystallographic data of the corresponding MBA molecule.[11-13]

Figure 2 (a) Cu K-edge XANES spectra of Cu/*o*-MBA/TiO_2(110) in three different polarization directions. (b) Cu K-edge XANES spectra of reference samples.

Figure 3 (a) Cu K-edge EXFAS spectra of Cu/*o*-MBA/TiO_2(110) in three different polarization directions. (b) Cu K-edge EXAFS spectra of reference samples.

Figure 4 (a) Proposed structure of Cu/*o*-MBA/TiO_2(110). (b) Cu K-edge EXAFS spectra, where the black solid and red dotted lines are the observed and calculated EXAFS oscillations, respectively. (Side and top views of the model structure and the selected atomic coordinates used for calculation are given in Supplementary Information (Figure S3 and Table S1, respectively).)

Figure 5 Cu K-edge (a) XANES and (b) EXAFS spectra of Cu/*m*-MBA/TiO_2(110) in three different polarization directions.

Figure 6 (a) Proposed structure of Cu/*m*-MBA/TiO_2(110). (b) Cu K-edge EXAFS spectra, where the black solid and red dotted lines are the observed and calculated EXAFS oscillations, respectively. (Side and top views of the model structure and the selected atomic coordinates used for calculation are given in Supplementary Information (Figure S4 and Table S2, respectively).)

Figure 7 Cu K-edge (a) XANES and (b) EXAFS spectra of Cu/*p*-MBA/TiO2(110) in three different polarization directions.

Figure 8 (a) Proposed structure of Cu/*p*-MBA/TiO_2(110). (b) Cu K-edge EXAFS spectra, where the black solid and red dotted lines are the observed and calculated EXAFS oscillations, respectively. (Side and top views of the model structure and the selected atomic coordinates used for calculation are given in Supplementary Information (Figure S5 and Table S3).)

Figures

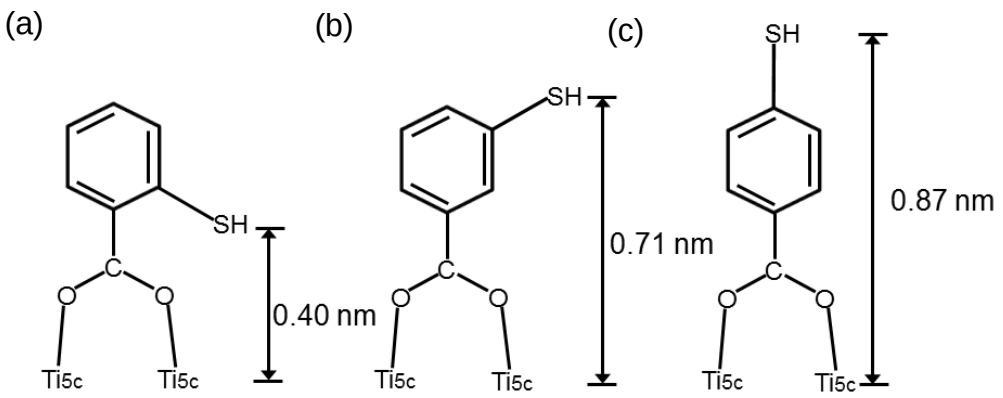

Figure 1 Structural models of (a) *o*-MBA, (b) *m*-MBA and (c) *p*-MBA adsorbed on a TiO_2(110) surface. Ti_{5c} denotes fivefold-coordinated Ti^{4+} of the TiO_2(110) surface. The distance of the S atom to the Ti_{5c} was estimated from the previous reports that are theoretical calculation of adsorbed structure of formate on the TiO_2(110) surface[10] and crystallographic data of the corresponding MBA molecule.[11-13]

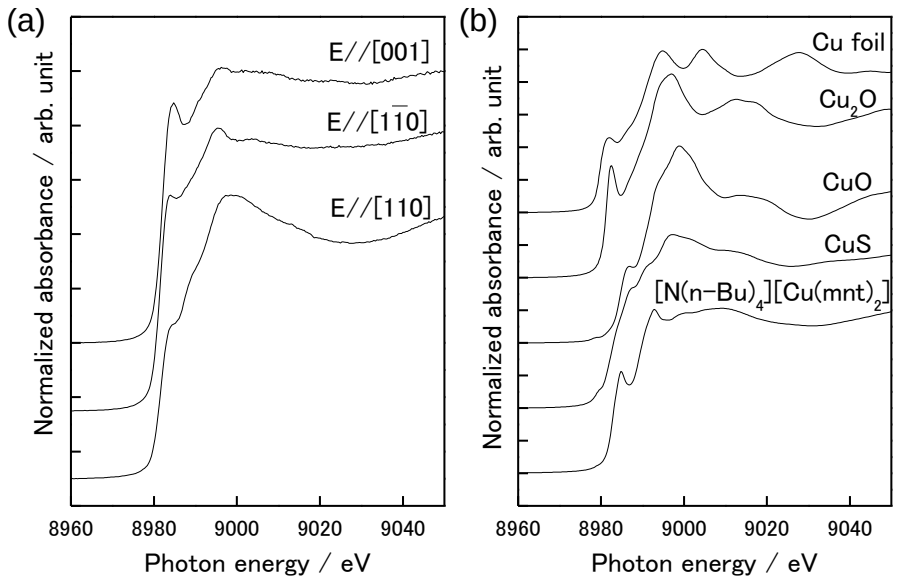

Figure 2 (a) Cu K-edge XANES spectra of Cu/*o*-MBA/TiO_2(110) in three different polarization directions. (b) Cu K-edge XANES spectra of reference samples.

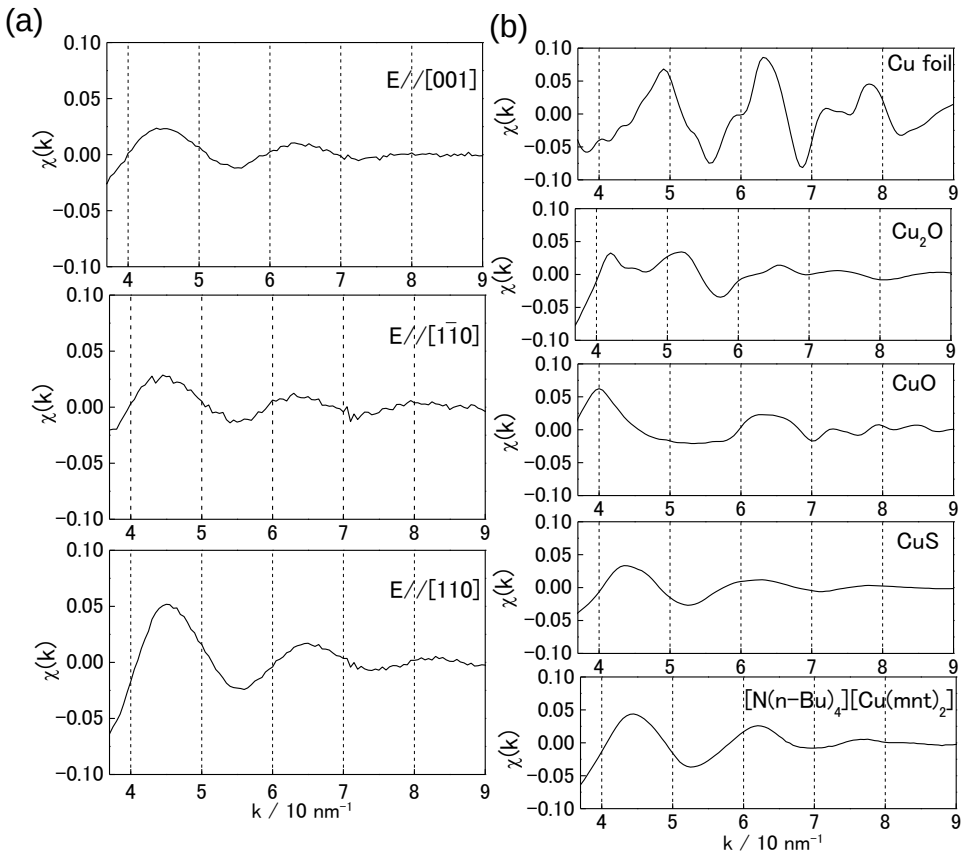

Figure 3 (a) Cu K-edge EXFAS spectra of Cu/*o*-MBA/TiO_2(110) in three different polarization directions. (b) Cu K-edge EXAFS spectra of reference samples.

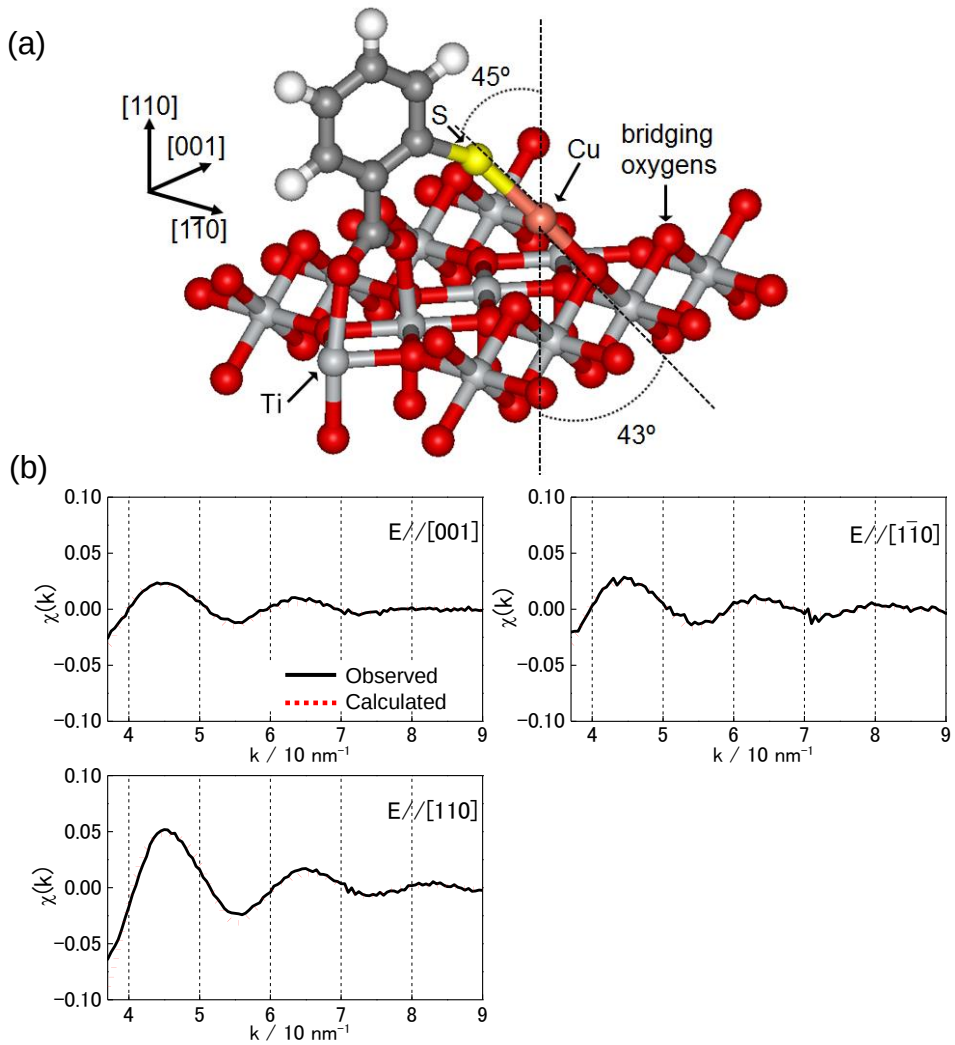

Figure 4 (a) Proposed structure of Cu/*o*-MBA/TiO_2(110). (b) Cu K-edge EXAFS spectra, where the black solid and red dotted lines are the observed and calculated EXAFS oscillations, respectively. (Side and top views of the model structure and the selected atomic coordinates used for calculation are given in Supplementary Information (Figure S3 and Table S1, respectively).)

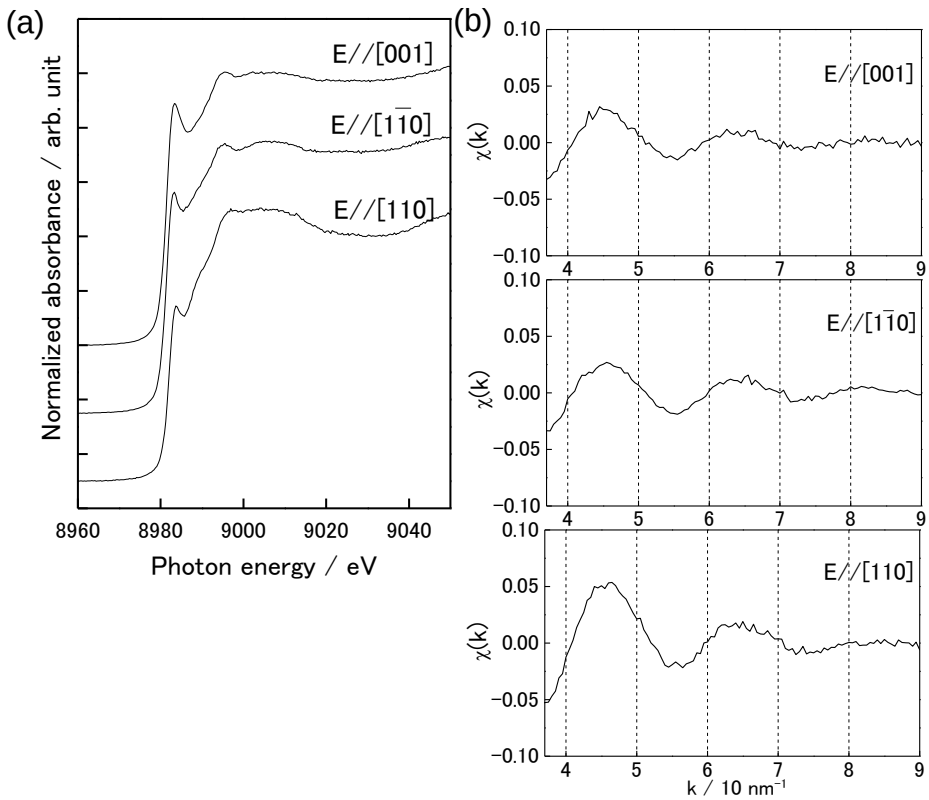

Figure 5 Cu K-edge (a) XANES and (b) EXAFS spectra of Cu/*m*-MBA/TiO_2(110) in three different polarization directions.

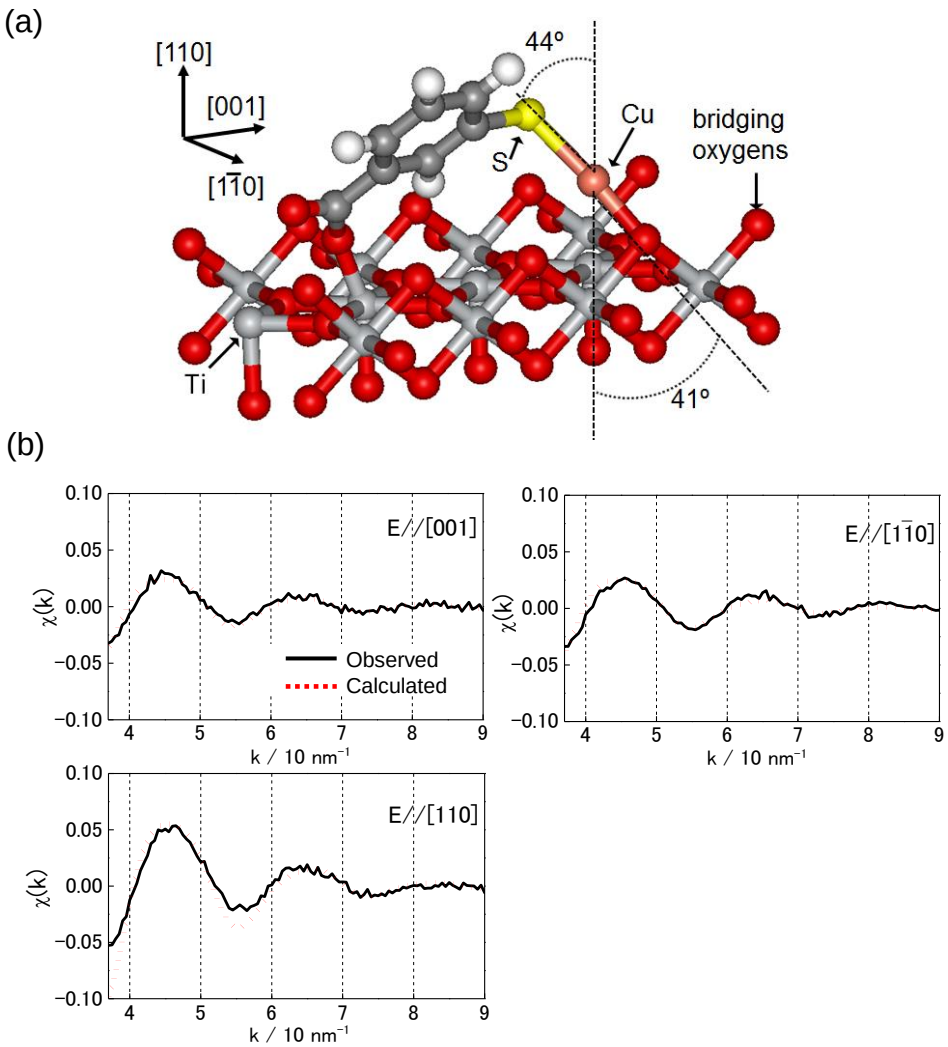

Figure 6 (a) Proposed structure of Cu/*m*-MBA/TiO_2(110). (b) Cu K-edge EXAFS spectra, where the black solid and red dotted lines are the observed and calculated EXAFS oscillations, respectively. (Side and top views of the model structure and the selected atomic coordinates used for calculation are given in Supplementary Information (Figure S4 and Table S2, respectively).)

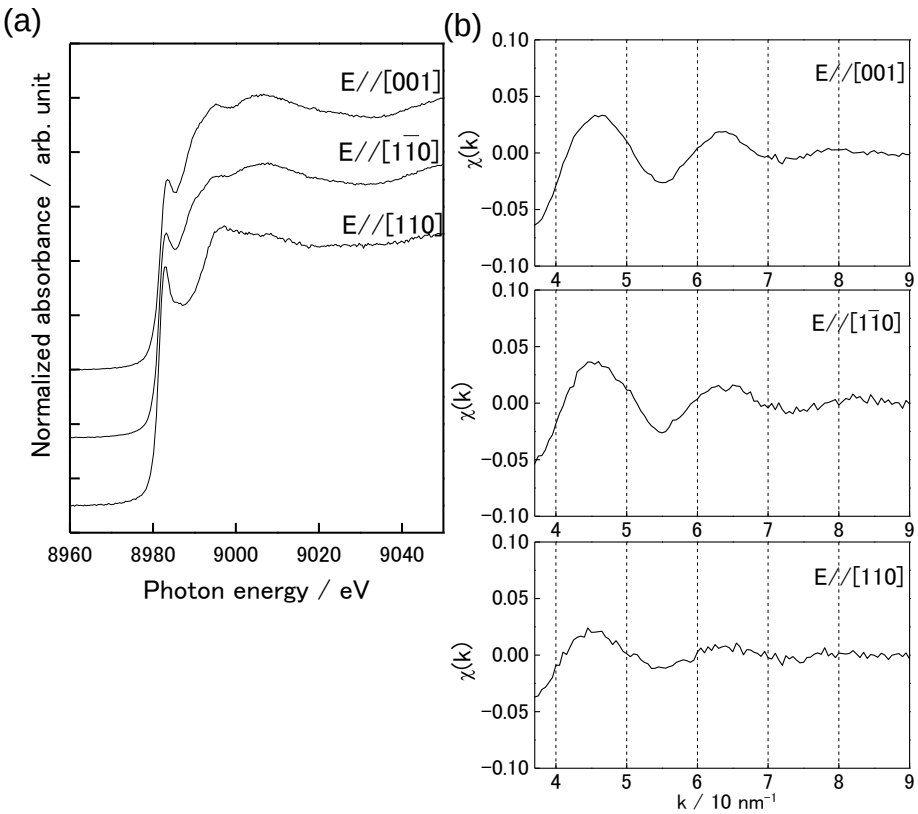

Figure 7 Cu K-edge (a) XANES and (b) EXAFS spectra of Cu/*p*-MBA/TiO_2(110) in three different polarization directions.

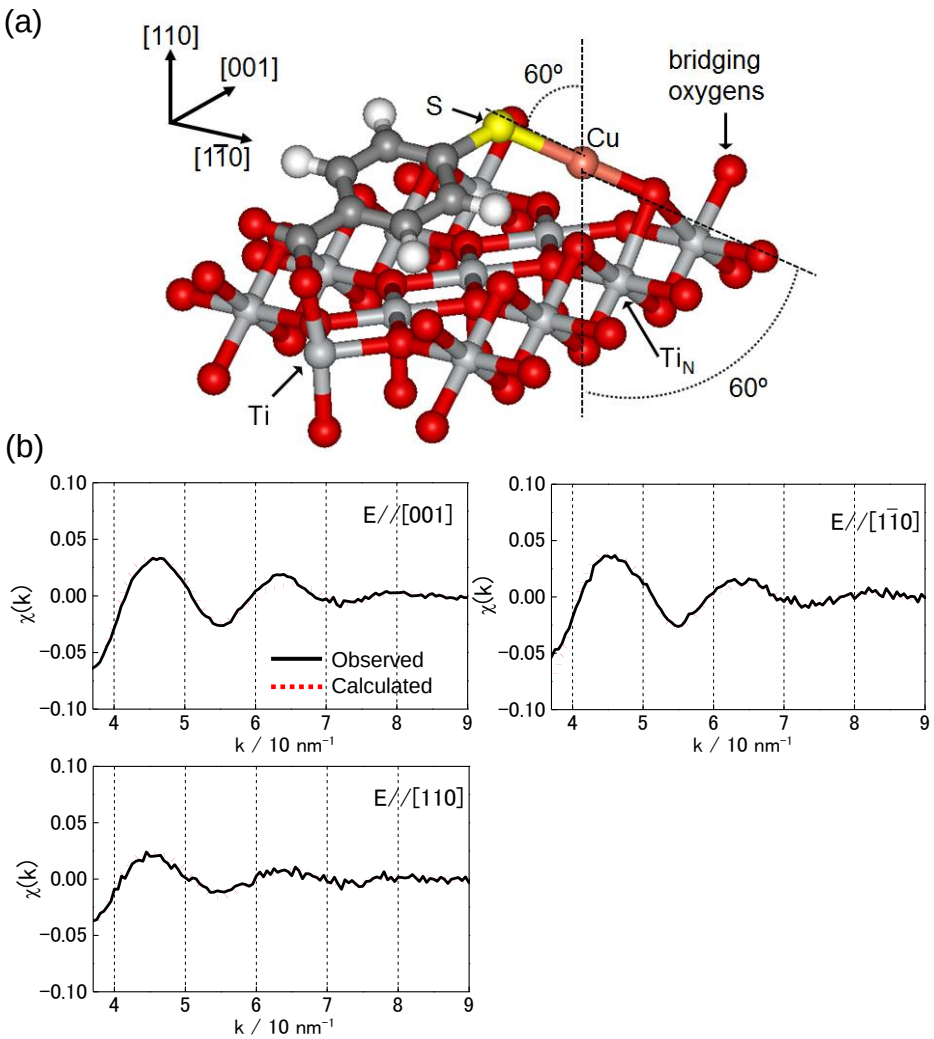

Figure 8 (a) Proposed structure of Cu/*p*-MBA/TiO_2(110). (b) Cu K-edge EXAFS spectra, where the black solid and red dotted lines are the observed and calculated EXAFS oscillations, respectively. (Side and top views of the model structure and the selected atomic coordinates used for calculation are given in Supplementary Information (Figure S5 and Table S3).)